Restorable Type Conversion of Carbon Nanotube Transistor Using Pyrolytically Controlled Antioxidizing Photosynthesis Coenzyme

By *Bo Ram Kang, Woo Jong Yu, Ki Kang Kim, Hyeon Ki Park, Soo Min Kim, Yongjin Park, Gunn Kim, Hyeon-Jin Shin, Un Jeong Kim, Eun-Hong Lee, Jae-Young Choi,** and *Young Hee Lee**

Here, a pyrolytically controlled antioxidizing photosynthesis coenzyme, β-Nicotinamide adenine dinucleotide, reduced dipotassium salt (NADH) for a stable n-type dopant for carbon nanotube (CNT) transistors is proposed. A strong electron transfer from NADH, mainly nicotinamide, to CNTs takes place during pyrolysis so that not only the type conversion from p-type to n-type is realized with 100% of reproducibility but also the on/off ratio of the transistor is significantly improved by increasing on-current and/or decreasing off-current. The device was stable up to a few months with negligible current changes under ambient conditions. The n-type characteristics were completely recovered to an initial doping level after reheat treatment of the device.

1. Introduction

Since several demonstrations of single-walled carbon nanotubes (SWCNTs) that revealed excellent transistor performances,[1–7] there have been tremendous efforts to utilize SWCNT transistors for practical circuit units with high integration density for the next generation after the silicon era.[8–11] Nevertheless, the development of the CNT technology has been hampered by several obstacles. One serious bottleneck technology is a precise doping control of CNTs for p-type[12] and more seriously for n-type. The doping concept of CNTs is very different from that of conventional semiconducting materials since the foreign impurity material is incorporated into the host material and the doping level is determined by the solubility of impurity materials within the host material. In contrast, all the host carbon atoms in SWCNTs are exposed to the nanotube surface or inner empty space, making them difficult to incorporate foreign atoms into substitutional or interstitial sites due to large activation energy. For this reason, doping of CNTs by the substitution of carbon atoms with foreign atoms such as nitrogen or boron has been rare let alone their control of the doping level.[13] Instead, adsorbates such as atoms, molecules, polymers with appropriate functional groups have been introduced on the nanotube surface.[13–18] The main effect is to-and-fro motion of electrons between adsorbates and CNTs that eventually causes the shift of the Fermi level.[19] The amount of electron transfer determines the doping level or the Fermi level of CNTs. Unlike a conventional metal-oxide-semiconductor field effect transistor (MOSFET) that involves a charge depletion layer, a CNT device is operated as a Schottky barrier FET in which the current is exclusively determined by the Schottky barrier engineering at the junction.[20] The direction of the transferred electrons decides the doping type. The n-type (p-type) doping is realized by electron transfer from adsorbates to CNTs (from CNTs to adsorbates) where the Fermi level is shifted towards the conduction (valence) band.

The p-type CNTs are naturally obtained under ambient conditions, presumably caused by the electron-accepting adsorbates that downshift the Fermi level towards the valence band. Similarly, n-type CNTs are obtained by the electron-donating adsorbates such as alkali metals and amine-rich polymers that upshift the Fermi level towards the conduction band.[21–23] However, n-type doping is realized after charge compensation of inherent hole carriers and hence difficult to achieve to reach high concentration of electron carriers. To make it worse, even though CNTs are n-doped, they are easily oxidized under ambient conditions.[24,25] Therefore, alkali metal doping is unstable in air.[24] Amine-rich polymers are degraded near the contacts at high

[*] Prof. Y. H. Lee, B. R. Kang, W. J. Yu, K. K. Kim, H. K. Park, S. M. Kim, Y. Park, Dr. G. Kim, H.-J. Shin
Sungkyunkwan Advanced Institute of Nanotechnology
BK21 physics division
Department of Energy Science
Center for Nanotubes and Nanostructured Composites
Sungkyunkwan University
Suwon 440-746 (Korea)
E-mail: leeyoung@skku.edu
Dr. J.-Y. Choi, H.-J. Shin
Display Device & Processing Laboratory
Samsung Advanced Institute of Technology
Suwon 449-712 (Korea)
E-mail: jaeyoung88.choi@samsung.com
Dr. U. J. Kim, Dr. E.-H. Lee
Frontier Research Laboratory
Samsung Advanced Institute of Technology
Suwon 449-712 (Korea)

DOI: 10.1002/adfm.200801712

source-drain voltages, restricting the range of operating voltages.[25] Furthermore, there have been few reports that revealed high on/off ratio in the transistor.

In this paper, we introduce β-Nicotinamide adenine dinucleotide, reduced dipotassium salt (NADH) as an n-dopant, a coenzyme found in all living cells that play a key biochemical role in metabolic redox reaction and in cell signaling, to reach high concentration of electron carriers with long time stability under ambient conditions. NADH was pyrolytically decomposed into NAD^+ and a proton at 150 °C. The nicotinamide group in NAD^+ played a key role in donating electrons to CNTs, whereas the adenine group was inert against charge transfer. The fabricated n-type transistors with NAD showed higher on/off ratios than those before n-doping. This was in good contrast with the conventional n-dopant with PEIs where relatively low on/off ratios were observed due to the high leakage current. Our devices were stable up to two months with a negligible change in the device characteristics under ambient conditions and fully recovered their device performance by reheat treatment. This environmentally free n-type doping enabled us to fabricate p–n junction diode and complementary inverter, and should be utilized to numerous complicated logic circuits.

2. Results and Discussion

NADH is an antioxidizing coenzyme found in all living cells that plays a key biochemical role in metabolic redox reactions and in cell signaling. It can reach high concentration of electron carriers with high stability. NADH consists of nicotinamide and adenine groups supported by ammonium dihydrogen phosphate (ADP)-ribose (Fig. 1a). NADH is a well-known reducing agent that generates electrons during one of the photosynthesis processes in living cells, where $NADH \leftrightarrow NAD^+ + 2\ e^- + H^+$.[26] The energy that is released during the oxidation of glucose, together with electrons and protons is transferred to NAD^+, resulting in the reduction of NADH, as part of glycolysis and the citric acid cycle. The electrons generated by the oxidation of NADH through glycolysis are transferred into the mitochondrion by the glycerol phosphate shuttle, which pumps protons across the membrane, generating ATP through oxidative phosphorylation.[27,28] A high NAD^+/NADH ratio allows this coenzyme to act as both an oxidizing agent and a reducing agent.[29] The strong reduction potential of NADH was utilized in imposing n-type doping in our SWCNT transistors.[30] One intriguing feature of NADH is that it has strong antioxidizing properties and thus prevents them from being oxidized under ambient conditions.[31,32] This provides a possibility for CNTs to maintain stable n-type characteristics under ambient conditions.

The prepared NADH solution described in the experimental method was simply dropped on an array of the SWCNT TFTs and *I*–*V* characteristics were measured (Fig. 1b–d).[33] Figure 1c shows the source-drain current (I_{DS}) as a function of gate bias (V_G) from the NADH-treated TFT. The I_{DS} increased at a positive V_G and was suppressed at a negative V_G with increasing drain bias (V_{DS}), clearly demonstrating n-type gate modulation. This is a remarkable change compared to the pristine sample that showed a clear p-type gate modulation (inset). The current was also well modulated with V_{DS}. The resulting on/off ratio was 10^4–10^5 with an off-current of 10^{-11}–10^{-9} A, depending on V_{DS}. I_{DS} increased almost linearly with V_{DS} and furthermore was well modulated by the gate bias.

As mentioned above, the nicotinamide in NADH (2*H*-nicotinamide) is transformed to that in NAD^+ (1*H*-nicotinamide) with a proton by oxidation and the release of two electrons during photodissociation (inset in Fig. 2a).[26,34] Unlike the conventional approach of spontaneous oxidization of NADH by ubiquinones,[34] the oxidation process of NADH by SWCNTs was endothermic. Therefore, NADH-decorated SWCNTs were pyrolytically controlled to transform NADH into NAD^+ and simultaneously generate electrons to donate to SWCNTs. UV absorption spectroscopy was used to monitor the oxidation of NADH by pyrolysis. An absorption maximum was observed near 340 nm from the NADH-dropped sample after drying at 40 °C (Fig. 2a). This absorption peak was significantly reduced after heat treatment at 150 °C. Our observation of an absorbance maximum near 340 nm in the absorption spectrum is consistent with previous reports[35,36] and enabled us to identify NADH with strong adsorption near 340 nm and NAD^+ with negligible adsorption. The effect of heat treatment in the SWCNT channel was clearly visible in Figure 2b and c. After a simple drying at 40 °C, the magnitude of I_{DS} was decreased by two orders of magnitude for an applied negative V_G compared to the as-prepared sample. The effectiveness of electron generation by the structural transformation of NADH to NAD^+ was poor in this case and hence

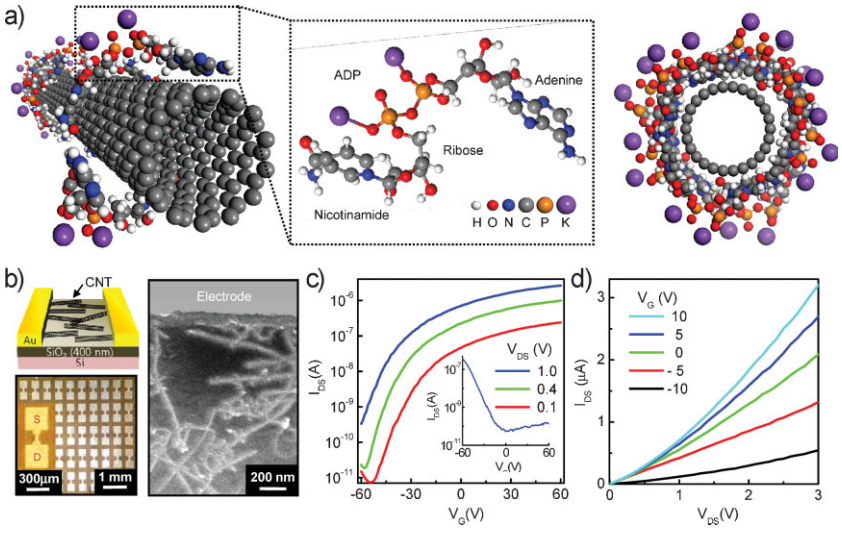

Figure 1. *I*–*V* characteristics of NADH-treated TFTs. a) Ball and stick model of NADH (middle) and the schematic of NADH adsorption of CNT surface (left) and front view (right). b) Schematic of SWCNT channel and the optical micrograph of a SWCNT array with a magnified channel with source and drain (left bottom). The corresponding SEM images of the SWCNT network in the channel. c) Typical I_{DS}–V_G characteristics of the NADH-treated device, showing n-type behavior (that of the pristine device in inset) and d) the corresponding I_{DS}–V_{DS} characteristics, showing an almost linear behavior.

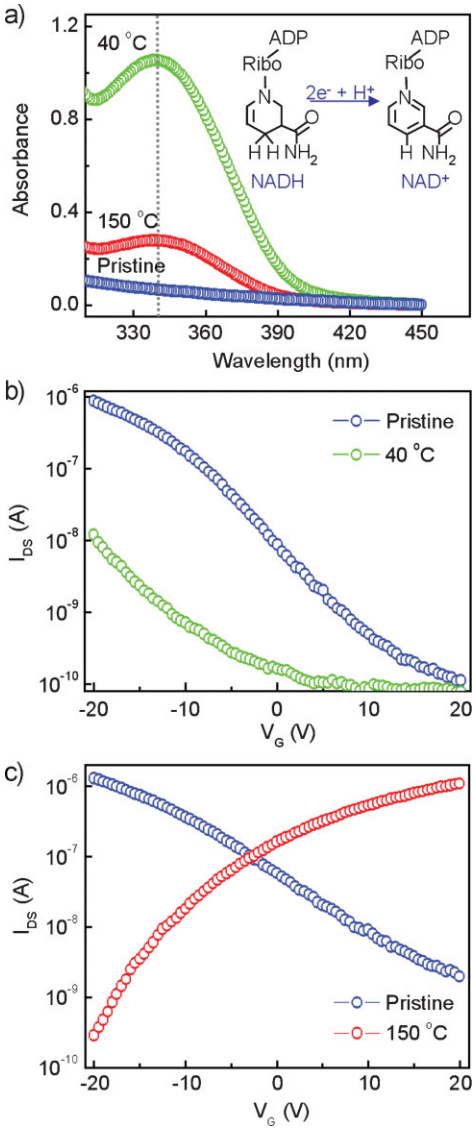

Figure 2. UV absorption of NADH-treated TFTs. a) UV absorption spectra of NADH-dropped SWCNTs (top), that of heat-treated sample at 150 °C for 3 min (middle), and that of the SWCNTs without adsorbates (bottom). The inset shows possible electron generation during the structure transformation. b) Typical *I*–*V* characteristics of the pristine SWCNT channel and that of an NADH-dropped channel after drying at 40 °C. c) The corresponding *I*–*V*s of the pristine sample and the sample after the NADH drop followed by heat treatment at 150 °C.

charge compensation partially occurred (Fig. 2b). However, with a heat treatment at 150 °C, NADH was fully converted to NAD^+, thus generating a high enough number of electrons. In this case, not only was there charge compensation, but type conversion was also clearly observed (Fig. 2c).

To estimate the electron-donating ability of NADH, we performed ab initio calculations based on the density functional theory. Because NADH consists of 2*H*-nicotinamide, presumably an electron-donating group,[37] we considered only a 2*H*-nicotinamide molecule adsorbed on a CNT. The optimized structure is provided in the bottom of Figure 3a. The circles indicate the 2H and 1H regions that are different structurally from each other. The binding energy of 2*H*-nicotinamide was –0.88 eV (exothermic) with a nearest separation distance of 2.53 Å. No practical charge transfer occurred during this adsorption. In contrast, neutral 1*H*-nicotinamide (Fig. 3b), which is a functional group of NAD, donated electrons to the CNT by 0.62 e. Due to another electron from reaction ($NADH \leftrightarrow NAD + e^- + H^+$), the net donated charges are 1.62 e. This ensures that carbon nanotubes can be an n-type semiconductor by doping with 1*H*-nicotinamide. Energy band structures of the 1*H*-nicotinamide and 2*H*-nicotinamide on the (8,0) nanotube show the same behavior (See the Supporting Information Fig. S1). For positively charged 1*H*-nicotinamide (See the Supporting Information Fig. S2), electrons are transferred from the CNT to nicotinamide by 0.23 e. However, two electrons generated during conversion ($NADH \leftrightarrow NAD^+ + H^+ + 2\ e^-$) from NADH to NAD^+ are expected to be transferred to CNTs and therefore total charges of 1.77 e are donated to the CNT, compared to 1.62 e in the neutral NAD. These results clearly showed the difference between 1*H*-nicotinamide and 2*H*-nicotinamide. In addition, the binding energy of 1*H*-nicotinamide increased to −1.46 eV with a closer nearest separation distance of 2.45 Å. The corresponding *I*–*V* characteristics with nicotinamide solution (not NADH) showed a type conversion from p-type to n-type after the same heat treatment (Fig. 3c and d). Similar calculations were done for the adenine group of NADH (see the Supporting Information Fig. S3). No practical charge transfer was observed, unlike the nicotinamide group. The corresponding *I*–*V* characteristics with an adenine solution also showed no type conversion before and after the same heat treatment (see the Supporting Information Fig. S3). Our additional experiments with theoretical analyses led us to conclude that it was the 1*H*-nicotinamide group, not the adenine group, that played an important role in donating electrons to the CNTs, causing the type conversion from p-type to n-type.

To investigate the doping efficiency, TFTs with various on/off ratios were doped. Relatively high on/off ratios were obtained even without electrical breakdown process. This demonstrated the efficiency of our approach in fabricating NxN channels compared to the previous works.[23,38] Remarkably, all the samples, independent of the on/off ratios, showed type conversion; furthermore, device performance was improved with higher on/off ratios, as observed in Figure 4a. It is of note that even the devices with low on/off ratios (large off-currents) were converted to n-type devices. Despite unpredictable doping probability in the network SWCNT TFTs, a high yield of type conversion was observed. We expect that the conversion efficiency should be improved in the case of isolated SWCNT device. Controllability of the doping concentration was also investigated. *I*–*V* characteristics were measured by increasing the number of droplets of the NADH solution onto the same channel (Fig. 4b). To see this effect, we used a low-concentration solution (1.35 mM) of NADH. Initially, p-type channels were gradually converted to n-type with increasing number of droplets. The hole current at a negative gate bias was drastically suppressed by the charge compensation, whereas the electron current at a positive gate bias increased gradually. The electron current again exceeded the hole current in this case, increasing on/off ratio. It is of note that the n-type carrier concentration was controlled precisely by increasing the number

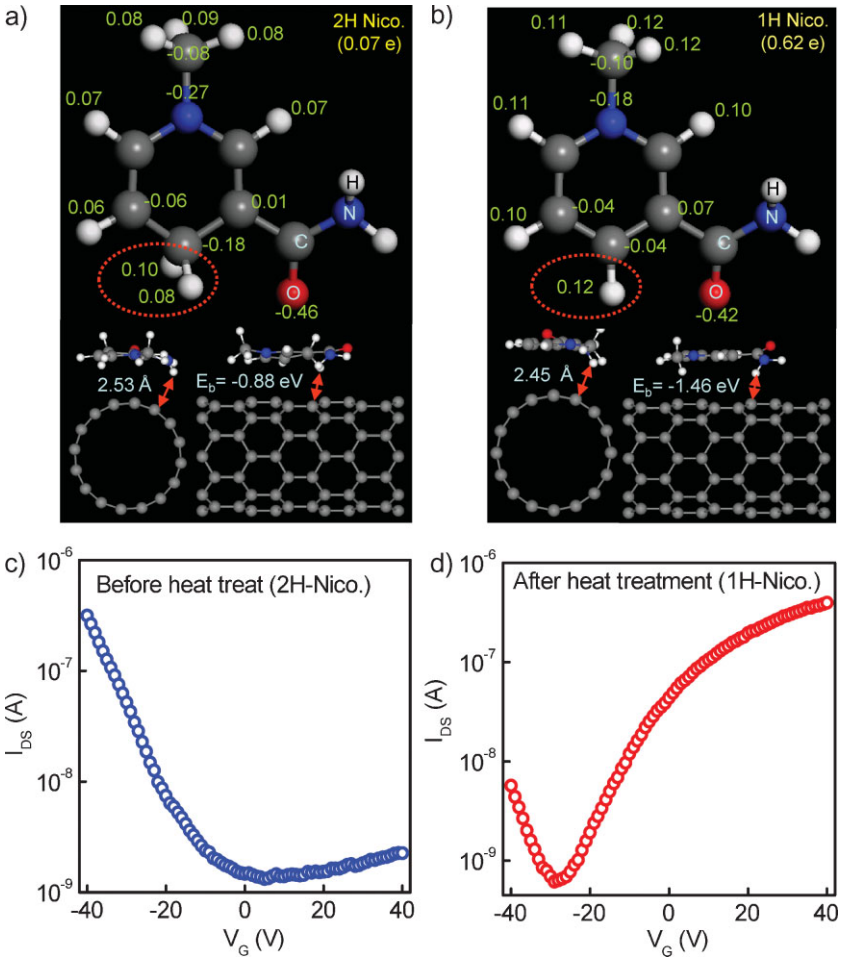

Figure 3. DFT calculations for charge transfer and binding energy of neutral nicotinamide. The optimized structures of a) 2*H*-nicotinamide and b) 1*H*-nicotinamide. The values indicate the amount of Mulliken charge on the nicotinamide after adsorption on CNT. Negative signs indicate the accumulation of electrons. The shortest separation distance is marked in the bottom panel with the binding energy. In the neutral 1*H*-nicotinamide, electrons are transferred from nicotinamide to CNT by 0.62 e. *I*–*V* characteristics c) before (2*H*-nicotinamide) and d) after (1*H*-nicotinamide) heat treatment.

of NADH droplets, which is another advantage of this approach compared to the conventional metal electrodes.[39]

Doping was conducted under ambient conditions for our experiments. A heavily-doped device was left under ambient conditions for up to two months. The on/off ratio was slightly reduced but the n-type doping behavior was still preserved (Fig. 4c). Another lightly-doped device was exposed for 100 days under ambient conditions and heat-treated again at 150 °C. The n-doped sample after 100 days was converted to p-type. However, n-type character was fully recovered to the similar level as the as-doped sample after re-heat treatment (Fig. 4d). This pyrolytically controlled bistability of n-type doping is in good contrast to the conventional n-type dopant of alkali metals that do not have controllability in the carrier concentration. The remarkably high stability was attributed to the presence of bulky ADP and ribose in NADH, acting as a protective layer, which could be an origin of antioxidant properties of NADH (right panel of Fig. 1a).[29,30] This was confirmed by the separate nicotinamide doping without the bulky part of ADP and ribose that showed relatively short term stability. This long term stability in NADH allowed fabrication of circuits using conventional lithography under ambient conditions. These circuits could be protected by a capping layer after completion. We expect that this reversible stability will prove to be advantageous in many aspects of device fabrication in the future.

In order to rationalize the better doping characteristics of NADH, the conventional PEI was further tested under similar situations. The on/off ratio after PEI treatment decreased to 10^2 from 10^4 (Fig. 5a). Figure 5b shows the long term stability of the PEI-doped sample. The current level was significantly reduced with reduced on/off ratio. This is an evidence of the reduction of electron carriers (charge compensation) due to the oxidation under ambient conditions. The similar heat treatment of this sample at 150 °C decreased the current level further, although the on/off ratio increased significantly. In other words, the device characteristics were severely altered after re-heat treatment. This is in good contrast with the fully reversible NADH doping under re-heat treatment. The enhancement of on/off ratio in the NADH doping resulted from the suppression of the off current as shown in Figure 5c. On the other hand, the PEI doping increased on current by about 10 times but the off (leakage) current was enhanced as well by about 1000 times. Thus, the on/off ratio decreased by about 100 times in the case of PEI doping. This was attributed to the formation of conducting paths through the PEI (dopant) coating layer. It is noted that linear PEI has a small energy gap (≈0.4 eV),[40] which is similar to that of semiconducting CNTs.

The long term stability of NADH shown above allowed us to fabricate several devices. We first demonstrated this by forming a p–n junction where the half of the channel was covered by a photoresist using photolithography followed by the NADH drops (Fig. 6a). In spite of network SWCNT TFTs, the device clearly showed off-current at a positive drain bias and high on current at negative drain bias, revealing excellent rectifying behavior. Another advantage of this approach is that NADH doping is compatible with conventional photolithography, because NADH is not soluble in organic solvents such as acetone and alcohol. This contrasts with the conventional n-dopant of PEI that can be easily dissolved in organic solvent which cannot be therefore used for conventional photolithography.[25] The complementary inverter was fabricated by combining p-type and n-type TFTs in the same array. The p-channel and n-channel was connected by Au wire by using a wire bonder (Fig. 6b). V_{out} was switched by sweeping the back gate bias (V_{in}). The controllability of the doping level in an individual channel, which is critical for practical applications, can

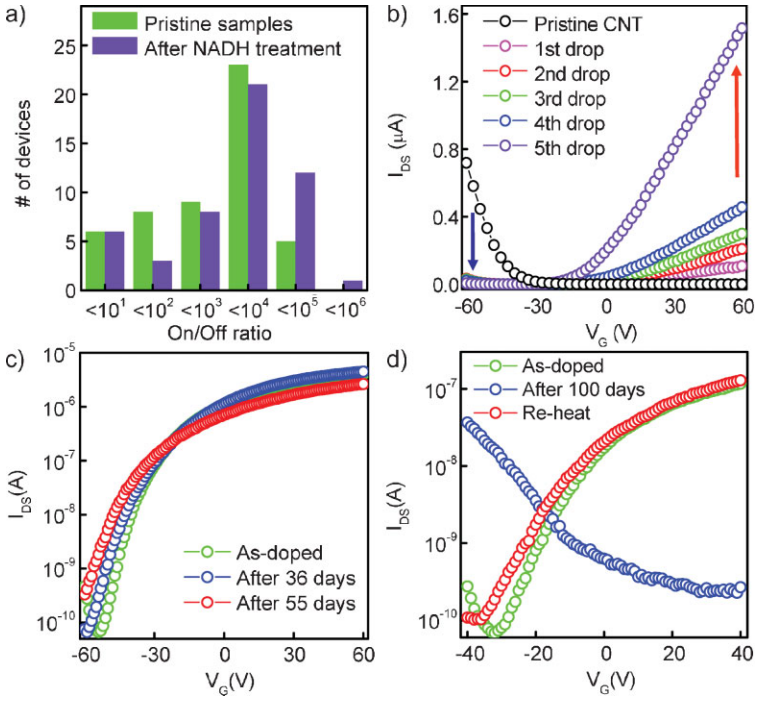

Figure 4. Controllability and stability of n-type doping. a) Statistics for the number of TFTs as a function of the on/off ratio before and after n-type doping. The total number of devices was 51. b) *I–V* characteristics in terms of number of NADH drops. Each drop of 100 μL had a concentration of 1.35 mM NADH. c) Stability of *I–V* characteristics of heavily doped device exposed for 36 and 55 days under ambient conditions. d) *I–V* characteristics of the lightly doped device after 100 days and after re-heat treatment at 150 °C.

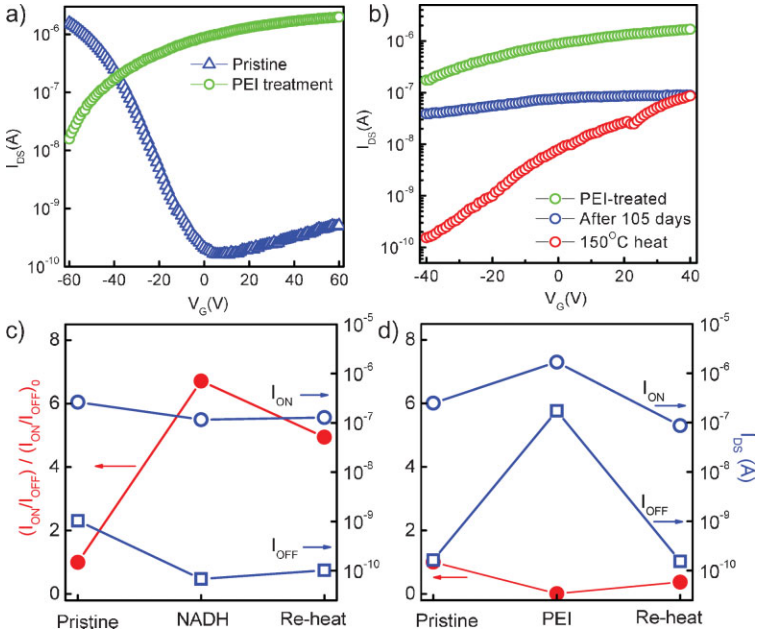

Figure 5. Comparison of NADH-treated sample to PEI-treated sample. a) I_{DS}–V_G characteristics of the pristine and NADH-treated sample and b) those of the pristine and PEI-treated sample. The variation of on/off ratio normalized by on/off ratio of the pristine sample, on current, and off current of c) NADH and d) PEI doping for the pristine, after doping, and re-heat treatment after 100 days.

be improved by adopting an ink jet printer, where droplet size can be controlled by the choice of nozzle size and doping solution.

3. Conclusions

In summary, we have demonstrated a method of implementing stable n-type doping of carbon nanotubes using antioxidizing photosynthesis coenzyme. The n-type doping was achieved by pyrolysis of NADH at 150 °C. The device characteristics such as on/off ratio and high on current/low off current were clearly demonstrated with controllability of doping concentration and 100% of doping yield. Long term stability of the n-doped CNT transistors up to two months was also observed. Together with density functional calculations, we found the follows. It was nicotinamide group, not adenine group in NAD that donated electrons to CNTs, invoking type conversion from p-type to n-type in CNT transistors. The long term stability originated from the backbone of NADH, namely ADP that played as a protecting layer against ambient oxidizing agents. Compared to these advantages, the conventional n-type dopant, PEI gave rise to undesirable device performance such as high leakage current and degradation of PEI near the contacts at high voltage. This long term stability enabled us to fabricate basic logic circuits under ambient conditions. We anticipate that our approach will allow fabrication of complicated CNT-based logic circuits and numerous device fabrications under ambient conditions.

4. Experimental

The network SWCNTs were synthesized with an array of predesigned pattern of photo-resist catalyst on Si substrate covered with SiO_2 (thickness: 400 nm) using plasma-assisted chemical vapor deposition. The corresponding source and drain electrodes with Ti (10 nm)/Au (100 nm) (channel length: 10 μm, width: 40 μm) were deposited to form an array of 200 thin film transistors. The detailed method has been described elsewhere [41]. NADH (98% purity), nicotinamide (99 + % purity), and adenine (99% purity) powders were purchased from Aldrich. NADH solutions of 13.5 mM, unless specified otherwise, were dissolved in deionized water followed by a sonication in a bath type for 30 min. Similarly, solutions of nicotinamide in deionized water and adenine in 1-methyl-2-pyrrolidinone (NMP) were obtained for comparison to NADH. One hundred microliters of the prepared solution was dropped onto ten TFT channels at a time by using a micropipette. Each sample was dried in an oven at 150 °C for 3 min.

Measurements: *I–V* characteristics of the CNT-TFTs were measured under ambient conditions by a source-measure unit (Keithley 236, 237) using a probe station. UV-vis-NIR absorption measurements were taken using a Cary 5000 spectrophotometer (Varian, CA, USA). For absorption measurements, the SWCNTs were prepared on quartz and the NADH solution was dropped. Scanning electron microscope (JEOL, JSM-7401F) images were taken by secondary electron image mode under a pressure of $\approx 4 \times 10^{-3}$ Torr.

Computational Methods: The first-principles pseudopotential calculations were performed based on the density functional

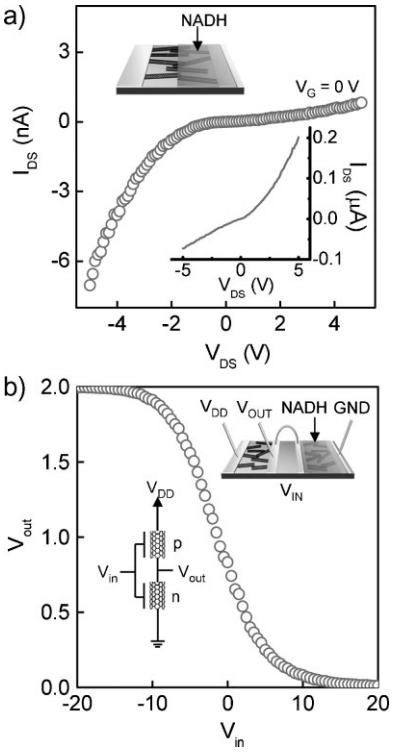

Figure 6. Fabrication of diode and inverter. a) *I–V* characteristics of a p–n junction diode fabricated by depositing an NADH solution on a half-covered TFT by photoresist. The top inset shows the schematic of the device and the bottom inset shows *I–V* characteristics of the pristine TFT. b) V_{in}–V_{out} characteristics of the inverter with the device schematic in the inset.

theory (DFT) within the local density approximation with the spin polarization (LSDA) implemented in the DMol3 package [42,43]. We used the double numerical basis set with a polarization p-function (DNP). Norm-conserving DFT semicore pseudopotentials were employed to describe the core and valance electrons [44–46]. A unit cell size of $20.00 \times 20.00 \times 17.04$ Å^3 for the (8,0) CNT, equivalently five unit cells, was chosen for total energy optimization. The total energy was calculated at the gamma point. The maximum forces were 0.002 Ha Å^{-1} with an energy convergency of 1.0×10^{-5} Ha during the geometry optimization. The binding energy of NADH was calculated as the difference of total energies between the adsorbed system and the separate species, E_b(NADH) = E(NADH+CNT) − E(NADH) − E(CNT).

Acknowledgements

B.R.K and W.J.Y. contributed equally to this work (this acknowledgement was inserted on 24.08.09, after online publication. The editorial office apologizes for any inconvenience caused). This work was supported by the MOE through the STAR-faculty project and TND project, WCU (World Class University) program through the Korea Science and Engineering Foundation funded by the Ministry of Education, Science and Technology (R31-2008-000-10029-0), the KICOS through a grant provided by MOST in 2007 (No. 2007-00202), and KOSEF through CNNC at SKKU. Supporting Information is available online from Wiley InterScience or from the author.

Received: November 3, 2008
Revised: February 26, 2009
Published online: June 18, 2009

[1] T. Du1rkop, S. A. Getty, E. Cobas, M. S. Fuhrer, *Nano Lett.* **2004**, *4*, 35.
[2] Z. Yao, C. L. Kane, C. Dekker, *Phys. Rev. Lett.* **2000**, *84*, 2941.
[3] A. Javey, H. Kim, M. Brink, Q. Wang, A. Ural, J. Guo, P. Mcintyre, P. McEuen, M. Lundstrom, H. J. Dai, *Nat. Mater.* **2002**, *1*, 241.
[4] S. J. Wind, J. Appenzeller, R. Martel, V. Derycke, P. Avouris, *Appl. Phys. Lett.* **2002**, *80*, 3817.
[5] B. M. Kim, T. Brintlinger, E. Cobas, M. S. Fuhrer, *Appl. Phys. Lett.* **2004**, *84*, 1946.
[6] S. Rosenblatt, Y. Yaish, J. Park, J. Gore, V. Sazonova, P. L. McEuen, *Nano Lett.* **2002**, *2*, 869.
[7] W. J. Yu, U. J. Kim, B. R. Kang, I. H. Lee, E. -H. Lee, Y. H. Lee, *Nano Lett.* **2009**, *9*, 1401.
[8] A. Bachtold, P. Hadley, T. Nakanishi, C. Dekker, *Science* **2001**, *294*, 1317.
[9] A. Javey, Q. Wang, A. Ural, Y. Li, H. J. Dai, *Nano Lett.* **2002**, *2*, 929.
[10] Z. Chen, J. Appenzeller, Y. M. Lin, J. Sippel-Oakley, A. G. Rinzler, J. Tang, S. J. Wind, P. M. Solomon, P. Avouris, *Science* **2006**, *311*, 1735.
[11] C. Kocabas, H. S. Kim, T. Banks, J. A. Rogers, A. A. Pesetski, J. E. Baumgardner, S. V. Krishnaswamy, H. Zhang, *Proc. Natl. Acad. Sci. USA* **2008**, *105*, 1405.
[12] W. J. Yu, S. Y. Jeong, K. K. Kim, B. R. Kang, D. J. Bae, M. Lee, S. Hong, S. P. Gaunkar, D. Pribat, D. Perello, M. Yun, J. Y. Choi, Y. H. Lee, *New J. Phys.* **2008**, *10*, 113013.
[13] D. L. Carroll, Ph. Redlich, X. Blase, J. C. Charlier, S. Curran, P. M. Ajayan, S. Roth, M. Rühle, *Phys. Rev. Lett.* **1998**, *81*, 2332.
[14] V. Derycke, R. Martel, J. Appenzeller, P. Avouris, *Appl. Phys. Lett.* **2002**, *80*, 2773.
[15] R. Martel, V. Derycke, C. Lavoie, J. Appenzeller, K. K. Chan, J. Tersoff, P. Avouris, *Phys. Rev. Lett.* **2001**, *87*, 256805.
[16] C. Klinke, J. Chen, A. Afzali, P. Avouris, *Nano Lett.* **2005**, *5*, 555.
[17] G. P. Siddons, D. Merchin, J. H. Back, J. K. Jeong, M. Shim, *Nano Lett.* **2004**, *4*, 927.
[18] K. H. An, Y. H. Lee, *Nano* **2006**, *1*, 115.
[19] A. M. Rao, E. Richter, S. Bandow, B. Chase, P. C. Eklund, K. A. Williams, S. Fang, K. R. Subbaswamy, M. Menon, A. Thess, R. E. Smalley, G. Dresselhaus, M. S. Dresselhaus, *Science* **1997**, *275*, 187.
[20] S. Heinze, J. Tersoff, R. Martel, V. Derycke, J. Appenzeller, P. Avouris, *Phys. Rev. Lett.* **2002**, *89*, 106801.
[21] C. Zhou, J. Kong, E. Yenilmez, H. J. Dai, *Science* **2000**, *290*, 1552.
[22] M. Shim, A. Javey, N. W. S. Kam, H. J. Dai, *J. Am. Chem. Soc.* **2001**, *123*, 11512.
[23] Y. Zhou, A. Gaur, S. H. Hur, C. Kocabas, M. A. Meitl, M. Shim, J. A. Rogers, *Nano Lett.* **2004**, *4*, 2031.
[24] V. Derycke, R. Martel, J. Appenzeller, P. Avouris, *Nano Lett.* **2001**, *1*, 453.
[25] S. H. Hur, C. Kocabas, A. Gaur, O. O. Park, M. Shim, J. A. Rogers, *J. Appl. Phys.* **2005**, *98*, 114302.
[26] D. L. Nelson, M. C. Michael, *Lehninger Principles of Biochemistry*, Worth Publishers, New York, USA **2000**.
[27] B. M. Bakker, K. M. Overkamp, A. J. van Maris, P. Kotter, M. A. Luttik, J. P. van Dijken, J. T. Pronk, *FEMS Microbiol. Rev.* **2001**, *25*, 15.
[28] P. R. Rich, *Biochem. Soc. Trans.* **2003**, *31*, 1095.
[29] D. G. Nicholls, S. J. Ferguson, *Bioenergetics 3*, Academic, London, UK **2002**.
[30] M. J. O'Connell, E. E. Eibergen, S. K. Doorn, *Nat. Mater.* **2005**, *4*, 412.
[31] M. Kirschi, H. D. Groot, *FASEB J.* **2001**, *15*, 1569.
[32] R. A. Olek, W. Ziolkowski, J. J. Kaczor, L. Greci, J. Popinigis, J. Antosiewicz, *J. Biochem. Mol. Biol.* **2004**, *37*, 416.
[33] The choice of CNT-TFTs synthesized by CVD was practical in our approach, since it provides numerous sets of devices for doping tests. The doping efficiency is supposedly poorer than that of individual devices. This method is fully adoptable for individual CNT device with better doping performance.
[34] P. Atkins, J. Paula, *Physical Chemistry, Oxford, UK* **2002**.

[35] M. C. Dawson, *Biochemical Research*, Oxford Scientific Publications, London, UK **1987**.
[36] U. Vitinius, K. Schaffner, M. Demuth, M. Heibel, H. Selbach, *Chem. Biodiversity* **2004**, *1*, 1487.
[37] P. Belenky, K. L. Bogan, C. Brenner, *Trends Biochem. Sci.* **2007**, *32*, 12.
[38] S. J. Kang, C. Kocabas, T. Ozel, M. Shim, N. Pimparkar, M. A. Alam, S. V. Rotkin, J. A. Rogers, *Nat. Nanotechnol.* **2007**, *2*, 230.
[39] Z. Zhang, X. Liang, S. Wang, K. Yao, Y. Hu, Y. Zhu, Q. Chen, W. Zhou, Y. Li, Y. Yao, J. Zhang, L. M. Peng, *Nano Lett.* **2007**, *7*, 3603.
[40] G. Herlema, B. Lekard, *J. Chem. Phys.* **2004**, *120*, 9376.
[41] Y. S. Min, E. J. Bae, B. S. Oh, D. Kang, W. Park, *J. Am. Chem. Soc.* **2005**, *127*, 12498.
[42] J. P. Perdew, Y. Wang, *Phys. Rev. B* **1992**, *45*, 13244.
[43] MATERIALS STUDIO (version 4.1) of Accelrys Inc., San Diego, USA.
[44] M. Ceperley, B. J. Alder, *Phys. Rev. Lett.* **1980**, *45*, 566.
[45] J. P. Perdew, A. Zunger, *Phys. Rev. B* **1981**, *23*, 5048.
[46] L. Kleinman, D. M. Bylander, *Phys. Rev. Lett.* **1982**, *48*, 1425.